Computational fluid dynamics modelling of solvent extraction equipment: A Review

K. K. Singh[1,2,*], Sourav Sarkar[1,2], Nirvik Sen[1], S. Mukhopadhyay[1,2], K.T. Shenoy[3]

[1]Chemical Engineering Division, BARC, Mumbai-400085, India

[2]Homi Bhabha National Institute, Anushaktinagar, Mumbai-400094, India

[3]Chemical Engineering Group, BARC, Mumbai-400085, India

Abstract

Solvent extraction is the most important separation process in nuclear fuel cycle. Different types of equipment are required for specific solvent extraction processes in the front-end and back-end of the nuclear fuel cycle. The complexity of the underlying phenomena (turbulent flow, multiphase flow, breakage and coalescence of droplets) renders design of solvent extraction equipment from first principles impossible. As a result, design of solvent extraction equipment is largely based on empirical correlations reported in literature, experimentation at different scales and operational experience. However, with availability of modelling tools like Computational Fluid Dynamics (CFD) and advancement in computational hardware, there is increasing thrust on thoroughly understanding the functioning of solvent extraction equipment aimed at optimal design, operation and scale-up. This article provides an overview of CFD modelling of solvent extraction equipment. The utility of single-phase CFD modelling in design of solvent extraction equipment which essentially involve multiphase flow is emphasized. Two-phase CFD modelling with the assumption of constant diameter monodispered droplets is discussed along with the governing equations and summary of some studies reported in literature. The necessity of coupling CFD and population balance modelling to capture the phenomena of continuously occurring breakage and coalescence of droplets to predict drop size along with the flow field is discussed. The approaches of population balance modelling and their governing equations are summarized. The need of interface tracking simulations for some solvent extraction equipment is discussed. The trends in using CFD modelling to predict mass transfer in solvent extraction equipment are also discussed.

Keywords: CFD, CFD-PBM, droplet, Euler-Euler, population balance, solvent extraction

Introduction

Solvent extraction is the most commonly used separation process in nuclear fuel cycle. The key processes using solvent extraction in nuclear fuel cycles are uranium refining, thorium processing, zirconium refining, and spent fuel reprocessing for closed fuel cycle [1, 2]. Solvent extraction is also used in several other processes of interest to the Department of Atomic Energy (DAE) such as production of rare-earth elements, value recovery from high level waste (HLW) for societal use, actinide partitioning in HLW, separation and purification of radioisotopes for radiopharmaceuticals and oncology [3-5].

Specific applications in nuclear fuel cycle require specific solvent extraction equipment. For example, one of the most important requirement of a solvent extraction equipment to be used in the back-end of the nuclear fuel cycle is that it should not have mechanical moving parts which require maintenance. This makes air pulsed columns very attractive for majority of applications in the back-end. However, in fast reactor fuel reprocessing, solvent degradation due to very high radiation field becomes the most important concern and the equipment which minimizes the contact time such as annular centrifugal extractor takes precedence over air pulsed column despite having part rotating at high speed. In the front-end of the nuclear fuel cycle, though maintenance is possible, passive equipment are still preferred. Another additional requirement a solvent extraction equipment has to fulfil to be worthy of deployment in the front-end is that it should be able to handle solids. The requirement of solid handling ability makes slurry extractor and pulsed disc and doughnut columns attractive in the front-end solvent extraction processes. In several applications in nuclear fuel cycle, the throughputs are too small which rule out the use of conventional solvent extraction equipment and special equipment that are ideal for low throughput applications such as Combine Air-lift Mixer-settler Unit (CALMSU) are required. On the contrary, in applications in which value has to be recovered from lean streams, very large throughputs are required which makes pump-mix mixer settlers and mechanically agitated columnar contactors such as rotating disc contactor (RDC) or asymmetric rotating disc contactor (ARDC) ideal. Thus, there is no solvent extraction equipment which can cater to all solvent extraction processes of interest in the nuclear fuel cycle.

The traditional way of designing solvent extraction equipment has been conducting experiments at bench-scale and pilot-scale and utilize the experimental data to design the equipment considering design margins. If conducting experiments is ruled

out, then the design is largely based on thumb rules and empirical correlations which have been reported extensively in literature for commonly used solvent extraction equipment. Operational experience with similar equipment is also heavily relied upon for designing solvent extraction equipment for new and/ or scaled-up facilities. In most cases, the scale-up followed in new facilities is incremental. The overwhelming reliance on experimentation, thumb rules, empirical correlations and operational experience is attributed to complexity of phenomena such as turbulent flow, multiphase flow, continuous brakeage and coalescence of droplets which are prevalent inside a solvent extraction equipment and which render mathematical modelling of solvent extraction equipment quite complex. However, traditional way of designing leads to significant design margins which must be avoided to reduce the capital and operating costs. Thus, there is growing need of using modelling tools such as Computational Fluid Dynamics (CFD) to thoroughly and fundamentally understand phenomena underlying solvent extraction equipment leading to optimized designs and confident scale-up while minimizing experimentation.

In nuclear fuel cycle, CFD is routinely used for design and thermal hydraulic analysis of nuclear reactors. But the application of CFD in the front-end and back-end of the nuclear fuel cycle, in which solvent extraction is arguably the most important unit operation, has lagged behind. However, in recent years, lot of work has been done on CFD modelling of solvent extraction equipment a glimpse of which is provided in this article to give an overview of the approaches used for and utility of CFD modelling of solvent extraction equipment relevant for nuclear fuel cycle.

Single-phase CFD modelling of solvent extraction equipment

Flow in a solvent extraction equipment is two-phase flow comprising of a liquid phase dispersed in another immiscible liquid phase. In some cases, three immiscible phases (for example, in air agitated liquid-liquid dispersion) or four immiscible phases (for example, in air agitated contactors in which feed contains solids) may also be present inside a solvent extraction equipment. The droplets in the liquid-liquid dispersion continuously undergo brakeage and coalescence. In addition to being two-phase or multiphase, flow is turbulent also. These complexities make CFD modelling of solvent extraction equipment quite complex. However, in several instances single-phase CFD modelling can help in design without going for very complex CFD model catering to all the phenomena prevalent in a solvent extraction equipment. CFD-assisted design of mechanically agitated mixers and pump-mix mixers is a very pertinent example of how single-phase CFD simulations can be useful for design of solvent extraction equipment. A mechanically agitated mixer is the basic equipment in a solvent extraction cascade comprising of mixer-settlers. The conventional method to design a mixer requires estimate of specific power input which can be estimated if the power number of the impeller to be used is known. Power number of conventionally used impellers (such as Rushton turbine, straight blade paddle, pitched blade turbine, propeller) are reported in literature. However, the reported values are for a specific geometric setting. The power number varies with varying impeller diameter to tank diameter ratio (D/T), impeller off-bottom clearance to tank diameter ratio (C/T), the blade width to impeller diameter ratio (B_w/D) etc. The dependence of power number on these geometric parameters can be significant. For example, on reducing C/T, a radial flow impeller such as Rushton turbine may start behaving as an axial flow impeller leading to a step reduction in power number on reducing the clearance [6]. The dependence of power number on the aforementioned geometric parameters is difficult to find in literature. Single-phase CFD simulations are very useful to estimate the power number of an impeller for such specific geometric setting.

In a mixer-settler cascade, the inter-stage pumping can be achieved by harnessing the pumping capacity of the rotating impeller itself instead of using inter-stage pumps. Such mixers, in which the impeller is expected to do the job of both mixing and inter-stage pumping, are called pump-mixers [7]. A mixer-settler based on pump-mixers is called pump-mix mixer-settler. The challenge in designing a pump-mix mixer is to identify a pump-mix

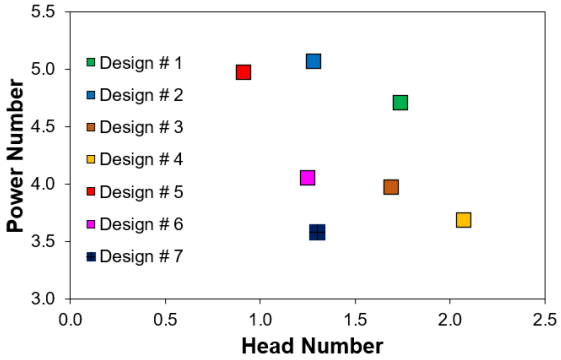

Fig.1: Power number and head number values of different designs of pump-mix mixers listed in Table 1.

Table 1: Different designs of pump-mix mixer for which single-phase CFD simulations were carried out to estimate head and power numbers as given in Fig. 1. (In all designs, the ratio of impeller diameter to tank diameter is 0.5, C/T represents impeller off-bottom clearance to tank diameter ratio, L_d/T represents the ratio of the length of the draft tube to tank diameter).

		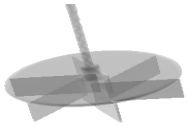	
Type-1 pump-mix impeller: Top-shrouded turbine having radial trapezoidal blades		Type -2 pump-mix impeller: Top-shrouded turbine having non-radial rectangular blades	
Design No.	Impeller type	C/T	L_d/T
1	Type-1	0.5	250/700
2	Type-1	0.5	115/700
3	Type-1	0.3	115/700
4	Type-2	0.3	115/700
5	Type-1	0.5	-
6	Type-1	0.3	-
7	Type-2	0.3	-

impeller which does the dual job of mixing and pumping satisfactorily. This requires knowledge of the power number as well head number of the pump-mix impeller. While power number data can be obtained from literature, the data on head number is almost non-existent. Also, the impellers used for pump-mix action are different from the impellers used for just mixing. For example, the pump-mix impeller are usually top-shrouded. The power number and head number data of such specialized impellers are not easily available in literature. Thus, single-phase CFD simulations for estimating power number and head number of pump-mix impeller being contemplated in design become very useful in designing a cascade of pump-mix mixer-settlers. For example, Fig.1 shows the power number and head number values predicted from single-phase CFD simulations of different designs of a pump-mix mixer described in Table 1. The pump-mix mixer (diameter = height = 700 mm) is to be designed to handle a total throughput of 4 m^3/hr with a residence time of 4 minute. Different designs involve two different types of impellers placed inside the mixing tank differently. First 4 designs have the provision of draft tube which is required to increase the pumping head. Fig. 1 can help select an appropriate design for a given mixing and pumping tasks. For example, Design # 4 is suitable if very high pumping head is required with mild mixing, whereas Design # 1 is suitable if high pumping head is required with high degree of mixing.

When throughputs to be handled are very high, meeting the pumping requirement without causing excessive mixing becomes a design challenge. In such cases, the impeller is placed close to the bottom of the mixer where the liquids are coming in. However, such a placement of impeller may cause poor mixing in the top part of the mixer causing the mixer to deviate from a well-mixed vessel. Single-phase CFD modelling can be used also to simulate the non-ideal mixing in such cases [7]. Single-phase CFD simulations of mixers and pump-mix mixer typically involve solving Reynolds Averaged Navier–Stokes (RANS) equations along with an appropriate set of equations to model turbulence. Standard k-e model is the most commonly used model of turbulence. Modelling of rotating impeller poses some challenges but over the years several techniques have been developed and incorporated in CFD solvers [8].

Single-phase CFD simulations are useful not only for mechanically agitated solvent extraction equipment but also for columnar solvent extraction equipment. In columnar equipment, it has been reported in literature that axial dispersion in single-phase flow is higher than in two-phase flow. Thus, the use of single-phase axial dispersion coefficient estimated from single-phase CFD modelling in conventional design procedure to predict mass transfer performance of the columnar contactor can give a working design while avoiding rigorous and hence complex two-phase simulations. Some of the single-phase CFD studies on solvent extraction equipment are summarized in Table 2.

Two-phase CFD modelling assuming monodispersed drops

The most common approach used to simulate liquid-liquid two-phase flow in a solvent extraction equipment is Euler-Euler

Table 2: Summary of some of the reported studies on single-phase CFD modelling of solvent extraction equipment. (PDDC: Pulsed Disc and Doughnut Column; APDDC: Annular Pulsed Disc and Doughnut Column; PSPC: Pulsed Sieve Plate Column; RDC: Rotating Disc Contactor)

Contactor	Turbulence model	Objectives
PDDC [9]	Standard *k-ε*	Understanding flow patterns, estimation of pressure drop and axial dispersion coefficient
APDDC [10]	Standard *k-ε*	Understanding flow pattern, estimation of pressure drop and axial dispersion coefficient
PDDC having different design of disc and doughnut type plates [11]	Standard *k-ε*	Understanding flow patterns, estimation of Peclet number, shear rate, turbulent energy dissipation rate and pressure drop per unit length for different designs of disc and doughnut internals
PSPC [12]	Standard *k-ε*	Understanding flow patterns, estimation of axial dispersion coefficient
Pump-mix mixer [13]	Standard *k-ε*	Estimation of head and power characteristics of pump-mix mixers
Pump-mix mixers [14]	Standard *k-ε*	Understanding flow patterns and estimation of head number, power number and prediction of RTD.
Pump-mix mixers [7]	Standard *k-ε*	Estimation of head and power characteristics of different designs of pump-mix impellers, thoroughly understand pump-mix action
RDC [15]	Standard *k-ε*, RNG *k-ε*, realizable *k-ε*, RSM	Understanding flow patterns and comparison of different turbulence models
PDDC [16]	Standard *k-ε*, RNG *k-ε*, Low Re *k-ε*, RSM	Understanding flow patterns and comparison of different turbulence model
PDDC [17]	Standard *k-ε*	Understanding flow patterns and estimation of axial dispersion coefficient.

approach. This approach is necessary as in a solvent extraction equipment the volume fraction of the dispersed phase is significant. In this approach, the continuity and momentum equations are solved separately for the dispersed phase and the continuous phase along with the equations of an appropriate model of turbulence. The equations of the continuous and dispersed phase are linked through the interphase momentum exchange term. The interphase momentum exchange in two-phase flow may be due to drag force, lift-force and added mass force. However, for liquid-liquid two-phase flow, drag force is considered the most important and in majority of two-phase CFD models of solvent extraction equipment reported in literature only drag force is considered to model interphase momentum exchange term. Similarly, mixture k-ε model is the most widely used turbulence model. In this model, turbulence is solved for the mixed phase rather than solving turbulence separately for individual phases using per-phase turbulence model. This helps in reduction in computational time. The Euler-Euler simulations require an estimate of drop diameter as drop diameter appears in the term used for quantification of the drag force. In reality, the diameter of the drops in a solvent extraction contactor is not constant as drops are continuously flowing and simultaneously undergoing breakage and coalescence. In fact, there always exists a drop size distribution. Thus, drop size distribution or at least average drop diameter should also be computed along with other flow variables. However, this approach is computationally demanding and often dispersed phase is assumed to have monodispersed drops having constant diameter. Thus, the drop diameter becomes a user input to the CFD model. As expected, the results of the CFD simulations depend on how good is the estimate of the drop diameter. The drop diameter to be used in the simulations can be based on the experimental measurements or it may be estimated from a suitable correlation reported in literature [18, 19]. A drag coefficient model is necessary to estimate the drag force to model interphase momentum exchange. One of several drag coefficient models reported in literature or available in CFD solver can be used to model interphase momentum exchange in liquid-liquid two-phase flow. Most of the reported drag models and drag models available in CFD solvers are empirical in nature and several of them are based on a single solid particle settling in quiescent liquid. Strictly speaking, use of such drag models in two-phase CFD models of solvent extraction equipment is not advisable as these models do not account for the presence of swarm of droplets, effect of turbulence and effect of internal circulation in the drops on the drag coefficient. For want of drag models which should be used for turbulent swarm of internally circulating droplets, the drag models which are strictly not applicable for turbulent liquid-liquid dispersion continue to be used for two-phase CFD modelling of solvent extraction equipment. As expected, the choice of the drag model may significantly affect the results of Euler-Euler CFD simulations [18]. This limitation of two-phase CFD models of solvent extraction equipment should be addressed by using CFD modelling to understand the effect of turbulence, internal circulation and presence of other droplets on the drag force exerted by the continuous phase on a droplet.

Table 3: Typical governing equations used for Euler-Euler two-phase simulations of solvent extraction equipment

$\nabla.(\phi_d\overrightarrow{u_d}+\phi_c\overrightarrow{u_c})=0$	Continuity equations	(1)
$\frac{\partial\phi_d}{\partial t}+\nabla.(\phi_d\overrightarrow{u_d})=\nabla.D_{md}\nabla\phi_d$		(2)
$\rho_c\frac{\partial\overrightarrow{u_c}}{\partial t}+\rho_c(\overrightarrow{u_c}.\nabla)\overrightarrow{u_c}=\nabla.\left[-p\bar{\bar{I}}+\bar{\bar{\tau}}_c\right]+\frac{\nabla\phi_c}{\phi_c}\bar{\bar{\tau}}_c+\rho_c\vec{g}+\frac{\overrightarrow{F_{m,c}}}{\phi_c}$	Momentum equation of the continuous phase	(3)
$\rho_d\frac{\partial\overrightarrow{u_d}}{\partial t}+\rho_d(\overrightarrow{u_d}.\nabla)\overrightarrow{u_d}=\nabla.\left[-p\bar{\bar{I}}+\bar{\bar{\tau}}_d\right]+\frac{\nabla\phi_d}{\phi_d}\bar{\bar{\tau}}_d+\rho_d\vec{g}+\frac{\overrightarrow{F_{m,d}}}{\phi_d}$	Momentum equation of the dispersed phase	(4)
$\bar{\bar{\tau}}_c=(\mu_c+\mu_T)\left(\nabla\overrightarrow{u_c}+(\nabla\overrightarrow{u_c})^T-\frac{2}{3}(\nabla.\vec{u}_c)\bar{\bar{I}}\right)-\frac{2}{3}\rho_c k\bar{\bar{I}}$	Closure for the continuous phase momentum equation	(5)
$\bar{\bar{\tau}}_d=(\mu_d+\mu_T)\left(\nabla\overrightarrow{u_d}+(\nabla\overrightarrow{u_d})^T-\frac{2}{3}(\nabla.\vec{u}_d)I\right)-\frac{2}{3}\rho_d k\bar{\bar{I}}$	Closure for dispersed phase momentum equation	(6)
$\overrightarrow{F_{m,c}}=\chi(\overrightarrow{u_d}-\overrightarrow{u_c})$	Equation for interphase force	(7)
$\chi=\frac{3\phi_d\phi_c\rho_c C_d\lvert u_d-u_c\rvert}{4d_{32}}$	Interphase exchange term	(8)
$C_d=max\left\{\frac{24}{Re_p}\left(1+0.15Re_p^{0.687}\right);0.44\right\}$	Equation for drag coefficient	(9)
$Re_p=\frac{\phi_c d_{32}\rho_c\lvert\overrightarrow{u_d}-\overrightarrow{u_c}\rvert}{\mu_c}$	Drop Reynolds number	(10)
$\rho_m\frac{\partial k}{\partial t}+\rho_m(\overrightarrow{u_m}.\nabla)k=\nabla.\left[\left(\mu_m+\frac{\mu_T}{\sigma_k}\right)\nabla k\right]+P_k-\rho_m\varepsilon$	Transport equation of turbulent kinetic energy for mixture *k-ε* model	(11)
$\rho_m\frac{\partial\varepsilon}{\partial t}+\rho_m(\overrightarrow{u_m}.\nabla)\varepsilon=\nabla.\left[\left(\mu_m+\frac{\mu_T}{\sigma_\varepsilon}\right)\nabla\varepsilon\right]+C_{1\varepsilon}\frac{\varepsilon}{k}P_k-C_{2\varepsilon}\rho_m\frac{\varepsilon^2}{k}$	Transport equation of turbulent energy dissipation rate for mixture *k-ε* model	(12)
$\rho_m=\phi_c\rho_c+\phi_d\rho_d$	Mixture density for use in mixture *k-ε* model	(13)
$\overrightarrow{u_m}=\frac{\phi_c\rho_c\overrightarrow{u_c}+\phi_d\rho_d\overrightarrow{u_d}}{\phi_c\rho_c+\phi_d\rho_d}$	Mixture velocity for use in mixture *k-ε* model	(14)
$\mu_T=\rho_m C_\mu\frac{k^2}{\varepsilon}$	Equation to estimate turbulent viscosity	(15)
$P_k=\mu_T\left[\nabla\overrightarrow{u_m}:(\nabla\overrightarrow{u_m}+(\nabla\overrightarrow{u_m})^T)-\frac{2}{3}(\nabla.\overrightarrow{u_m})^2\right]-\frac{2}{3}\rho_m k\nabla.\overrightarrow{u_m}$	Source term for turbulent kinetic energy in mixture *k-ε* model	(16)

ϕ_d: dispersed phase volume fraction; $\overrightarrow{u_d}$: dispersed phase velocity vector; ϕ_c: continuous phase volume fraction; $\overrightarrow{u_c}$: continuous phase velocity vector; t: time; $\bar{\bar{I}}$: Identity tensor; $\overrightarrow{F_{m,c}}$: Volumetric interphase force on continuous phase; $\overrightarrow{F_{m,d}}$: Volumetric interphase force on dispersed phase; $\bar{\bar{\tau}}_c$: Continuous phase stress tensor; $\bar{\bar{\tau}}_d$: Dispersed phase stress tensor; D_{md}: Turbulent dispersion coefficient; μ_c: Continuous phase viscosity; μ_d: Dispersed phase viscosity; μ_T: Turbulent viscosiy; p: Pressure; $\vec{g}$: Acceleration due to gravity; ρ_c: Continuous phase density; ρ_d: Dispersed phase density; C_d: Drag coefficient; Re_p: Droplet Reynolds number; P_k: Rate of generation of turbulent kinetic energy; d_{32}: Sauter mean drop diameter; k: Turbulent kinetic energy; ε: Turbulent energy dissipation rate; $\overrightarrow{u_m}$: Mixture velocity; ρ_m: Mixture density; $C_{1\varepsilon}$, $C_{2\varepsilon}$, C_μ, σ_k, σ_ε : Constants of mixture *k-ε* model of turbulence.

Table 3 lists the equations typically solved in Euler-Euler CFD model of a solvent extraction equipment. CFD simulations based on Euler-Euler approach assuming monodispersed droplets can help estimate spatial variations and average value of dispersed phase holdup. With drop diameter known, specific interfacial area can be estimated by using dispersed phase holdup. With specific interfacial area and dispersed phase holdup known, mass transfer can be estimated by using suitable correlations of mass transfer coefficient along with thermodynamic data. In case, the equipment is suspected to have significant deviation from ideal flow behaviour (which is the case more often than not), virtual residence time distribution experiments can also be carried out using CFD modelling to predict axial dispersion coefficient of the continuous phase and dispersed phase. This requires solving species transport equations for each phase. If the flow is steady, the species transport can be solved without simultaneously solving the flow field. In such case, the CFD simulations will comprise of two steps. In the first step, flow is solved and in the second step the species transport equations are solved utilizing the flow field solved in the first step. If the flow is inherently transient, as in air pulsed columns, species transport equations need to be simultaneously solved along with two-phase flow equations.

As an illustration, Fig. 2 shows the results of Euler-Euler two-phase simulations of Pulsed Disc and Doughnut Column (PDDC) reported in a recent study [20]. The study reported two-phase CFD modelling of PDDC using Euler–Euler approach assuming monodispersed drops to predict flow field and dispersed phase holdup. Drop diameter used in the CFD model was estimated from a correlation reported in literature. Further,

Table 4: Summary of some of the reported studies on Euler-Euler approach based two-phase CFD modelling of solvent extraction equipment assuming monodispersed drops. (RDC: Rotating Disc Contactor, ARDC: Asymmetric Rotating Disc Contactor, ARIC: Asymmetric Rotating Impeller Contactor)

Contactor	Turbulence model	Source of drop diameter	Drag model	Objective
PSPC [18]	mixture *k-ε*	Experimental data	Schiller–Naumann, Morsi–Alexander, Symmetric, Barnea–Mizrahi, Kumar–Hartland, Augier et al.	Estimation of dispersed phase holdup
PSPC [19]	mixture *k-ε*	Correlation	Kumar–Hartland, modified Kumar–Hartland	Estimation of dispersed phase holdup
PDDC [20]	mixture *k-ε*	Correlation	Schiller–Naumann	Estimation of dispersed phase holdup
PDDC [21]	mixture *k-ε*	Correlation	Schiller–Naumann	Estimation of dispersed phase holdup and Peclet number of both phases
RDC [15]	Realizable *k-ε*, RSM	Experimental data	Schiller-Naumann	Understanding flow pattern and comparison of turbulence models
APDDC [22]	mixture *k-ε*	Experimental data	Ishii and Zuber	Estimation of dispersed phase holdup
APDDC [23]	mixture *k-ε*	Experimental data	Ishii and Zuber	Estimation of dispersed phase holdup and axial dispersion coefficient of continuous phase
ARDC, ARIC [24]	mixture *k-ε*	Experimental data	Kumar- Hartland	Estimation of dispersed phase holdup
RDC [25]	Realizable *k-ε*	Experimental data	Schiller-Naumann	Estimation of dispersed phase holdup
Hybrid PSPC [26]	Realizable *k-ε*	Experimental data	Schiller-Naumann	Estimation of dispersed phase holdup and axial dispersion coefficient of continuous phase

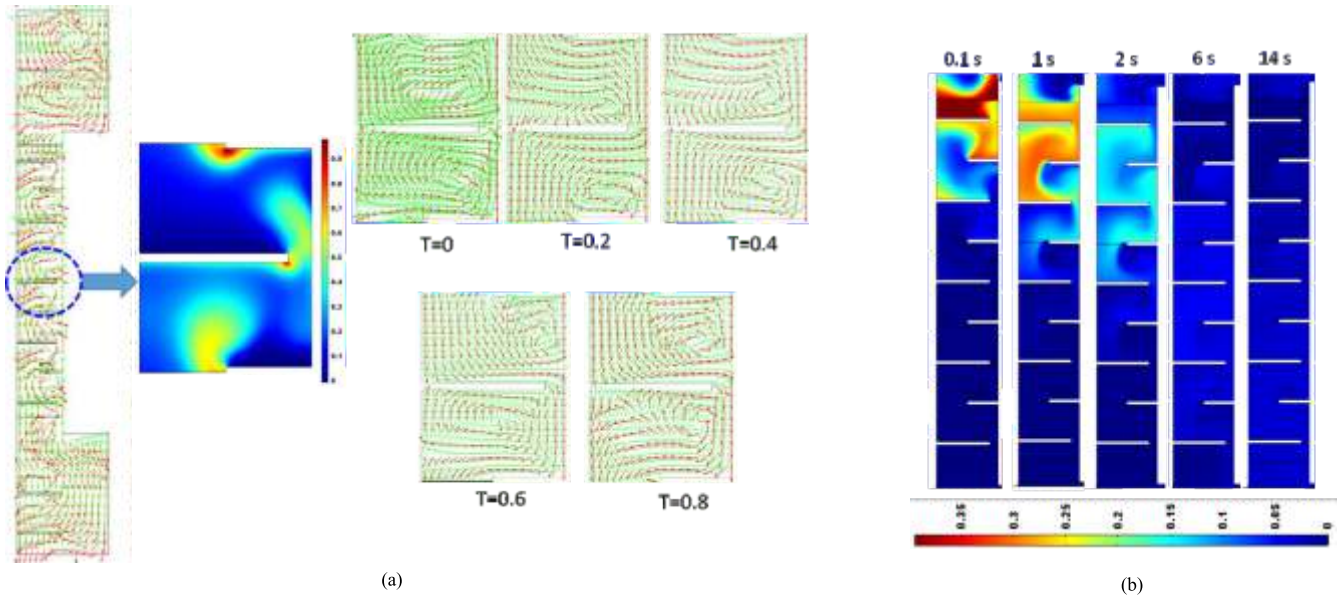

Fig. 2: (a) Typical velocity vectors of continuous and dispersed phase, dispersed phase holdup profile in an inter-disc space and velocity vectors of both phases in an inter-disc space at different instants of a pulsing cycle, (b) Typical progression of tracer in the computational domain with time in CFD-based RTD studies. "Reprinted with permission from {Sarkar et al., CFD modelling of pulsed disc and doughnut columns: prediction of axial dispersion in two-phase flow, Industrial & Engineering Chemistry Research, 2019, 58, 33, 15307-15320}. Copyright {2019} American Chemical Society."

it also reported solution of species transport equation along with the equations of Euler-Euler approach to obtain residence time distribution (RTD) of the continuous phase for estimation of axial dispersion coefficient or Peclet number of the continuous phase. Validation was done by comparing predicted and experimentally measured dispersed phase holdup, residence time distribution and Peclet number of the continuous phase for different dispersed phase velocities, continuous phase velocities and pulsing velocities. Table 4 summarizes some of the two-phase CFD studies on Euler-Euler simulations of solvent extraction equipment carried out by assuming monodispersed droplets.

Computational Fluid Dynamics – Population Balance Modelling

The CFD modelling approach discussed in the previous section is based on the assumption of monodispersed drops. Though, the assumption is often essential to simplify CFD model and reduce computational time, with this assumption phenomena of breakage and coalescence of drops which occur everywhere inside a solvent extraction equipment are not captured. The CFD model can be improved by doing away with this assumption by solving population balance equations along with the flow equations. This modelling approach is called as Computational Fluid Dynamics – Population Balance (CFD-PB) modelling. The modelling approach is schematically shown in Fig. 3. The solution of flow equations provides local values of the velocities of the two phases, dispersed phase holdup and turbulent energy dissipation rate which are utilized for solution of population balance equations. Solution of population balance equations provides local drop size distribution which can be used to obtain local value of an average diameter (most often Sauter mean diameter) which is used in the interphase momentum exchange term of the momentum equations of the Euler-Euler model. There are two widely used methods to solve the population balance equations. The first method is the method of classes. In the method of classes, the expected size range of the drops (e.g. 0-2000 μm) is divided into several classes. Each class has a size range and all the drops having size in that range are assumed to have a single size (representative class size). A population balance equation is solved for each class along with the equations of the Euler-Euler CFD model summarized in Table 3. The population balance equation for the drops having class diameter L is given in Table 5. The population balance equation is essentially a convection-diffusion equation with source and sink terms. The diffusion is often neglected. The source terms correspond to the generation of drops of that particular class due to breakage of drops of larger diameter classes and coalescence of the droplets of smaller diameter classes. The sink terms are due to loss of drops of the drop class because of their breakage and coalescence with drops of other drop classes. The source and sink terms require the kernels of breakage rate, coalescence rate and daughter droplet distributions. These kernels, based on empirical or semi-empirical models, are reported in literature [27]. Table 6 lists a set of often-used kernels. The solution of population balance equation gives the population of droplets in each class and hence the drop size distribution which can be used to obtain average droplet diameter. Sauter mean diameter is often used as the average droplet diameter. The Sauter mean diameter is used in the interphase momentum exchange term of the two-phase flow equations. The turbulent energy dissipation rate and dispersed phase holdup obtained from CFD simulations are used in the population balance equations. The method of classes is computationally expensive as one additional equation is solved along with two-phase flow equations for each drop class considered. For example, 10 additional equations will be solved along with the two-phase flow equations if the droplet size range expected in the solvent extraction equipment is discretized into 10 drop classes. To overcome this, another method called as the method of moments is used to solve the population balance. In this method, the transport equations of the moments of the drop size distribution are solved instead of the transport equations for the number density of the droplets. The typical equations of the method of moments are given in Table 7. This approach is computationally less expensive than the method of classes as only first three moments of the drop size distribution are of practical significance. Thus, only three equations representing the first three moments of the drop size distribution need to be solved along with the flow equations. The Sauter mean diameter to be used in the momentum equations can be obtained from the ratio of the third and the second moments of the drop size distribution. As in the method of classes, in the method of moments too, the source and sink terms representing breakage and coalescence are present in the transport equations.

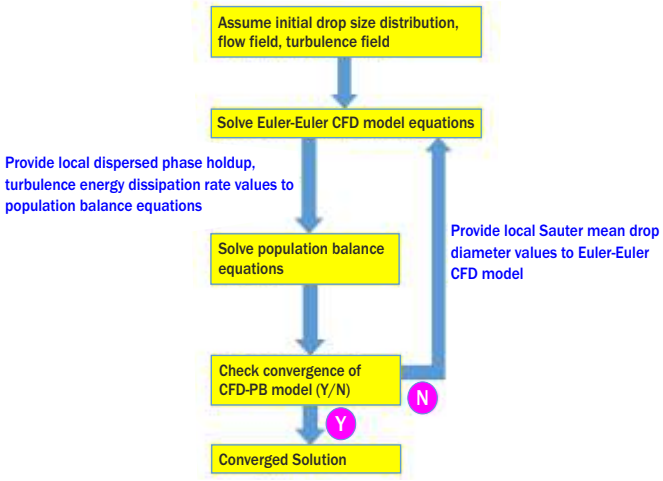

Fig. 3: Schematic of workflow in a CFD-PB model of solvent extraction equipment

CFD-PB model helps predict dispersed phase holdup, drop size and hence specific interfacial area. Axial dispersion coefficient can also be estimated by solving species transport along with the equations of CFD-PB model. Thus, CFD-PB model can provide estimates of all hydrodynamic variables which are required to predict mass transfer performance of a solvent extraction equipment. Population balance is an area of extensive research. Several new approaches to solve population balance equations in computationally efficient manner have been reported [28, 29].

Fig. 4 shows some results from a recently reported study on CFD-PB modelling of pulsed sieve plate column [30]. Method of classes was used for solving population balance equations. Validation was done by comparing predicted and measured dispersed phase holdup and Sauter mean drop diameter for different pulsing velocities and dispersed phase velocities. Validated CFD-PB model was used to have detailed insights into two-phase hydrodynamics such as axial variation of Sauter mean diameter and turbulent energy dissipation rate and spatial variations of Sauter mean diameter, turbulent energy dissipation rate, turbulent intensity, coalescence rate, Kolmogorov length scale between two sieve plates (shown in Fig. 4). Table 8 summarize some of the studies in which CFD-PB modelling of solvent extraction equipment has been reported. The approach

Table 5: Typical population balance equation solved along with Euler-Euler CFD model in method of classes to predict drop size distribution [30].

$\frac{\partial}{\partial t}\{n(L;t)\} + \nabla.(\overrightarrow{u_d}.n(L;t)) = B^b - D^b + B^c - D^c$	Convection-diffusion equation of population of drops of diameter L	(17)
$B^b = \int_L^\infty \upsilon(\lambda)\beta(L\|\lambda)a(\lambda)\, n(\lambda;t)d\lambda$	Source term for the birth of drops of diameter L due to breakage of larger drops	(18)
$D^b = a(L)n(L;t)$	Sink term for the death of drops of diameter L due to breakage	(19)
$B^c = \int_0^{L/\sqrt[3]{2}} h\{(L^3-\lambda^3)^{1/3},\lambda\}n\{(L^3-\lambda^3)^{1/3};t\}n(\lambda;t)d\lambda$	Source term for the birth of drops of diameter L due to coalescence of smaller drops	(20)
$D^c = n(L;t)\int_0^\infty h(L,\lambda)n(\lambda;t)d\lambda$	Sink term for the death of drops of diameter L due to coalescence with drops of other sizes	(21)
$d_{32} = \frac{\int_0^\infty L^3 n(L;t)dL}{\int_0^\infty L^2 n(L;t)dL}$	Expression to evaluate Sauter mean diameter from drop size distribution.	(22)
$n(L;t)$: Number of drops of diameter L at time t per unit volume of dispersion; $\overrightarrow{u_d}$: Dispersed phase velocity vector; t: time; B^b: Source term for birth of drops of diameter L due to breakage of larger drops; D^b: Sink term for death of drops of diameter L due to their breakage into smaller drops; B^c: Source term for birth of drops of diameter L due to coalescence of smaller drops; D^c: Sink term for death of drops of diameter Ldue to coalescence with other drops; $a(L)$: Breakage rate of drops of diameter L; $h(L,\lambda)$: Coalescence rate of droplets of diameter L and λ; $\beta(L\|\lambda)$: Distribution of daughter drops produced due to breakage of a drop of size λ; d_{32}: Sauter mean drop diameter; $\upsilon(\lambda)$: number of drops formed due to breakage of a drop of diameter λ.		

Table 6: Typical breakage, coalescence and daughter droplet distribution models used to define the source and sink terms of population balance equation [31].

$a(L) = C_1\frac{\varepsilon^{1/3}}{(1+\phi_d)L^{2/3}}\exp\left\{-C_2\frac{\sigma(1+\phi_d)^2}{\rho_d\varepsilon^{2/3}L^{5/3}}\right\}$	Breakage rate kernel defining rate of breakage of drops of diameter L	(23)
$h(L,\lambda) = \gamma(L,\lambda)\eta(L,\lambda)$	Coalescence rate kernel defining the rate of coalescence between drops of size L and λ. This is a product of collision rate and coalescence efficiency.	(24)
$\gamma(L,\lambda) = \left[C_3\frac{\varepsilon^{1/3}}{(1+\phi_d)}(L+\lambda)^2\left(L^{2/3}+\lambda^{2/3}\right)^{1/2}\right]$	Collision rate to model the rate of collision between droplets of size L and λ	(25)
$\eta(L,\lambda) = \exp\left\{-C_4\frac{\mu_c\rho_c\varepsilon}{\sigma^2(1+\phi_d)^3}\left(\frac{L\lambda}{L+\lambda}\right)^4\right\}$	Coalescence efficiency kernel to estimate the fraction of collisions between drops of size L and λ resulting in coalescence	(26)
$\beta(L\|\lambda) = 30\left(\frac{L^3}{\lambda^3}\right)\left(1-\frac{L^3}{\lambda^3}\right)$	Distribution of daughter drops produced due to breakage of a drop of diameter λ	(27)
ε: Turbulent energy dissipation rate; σ: Interfacial tension; C_1-C_4: Constants in the breakage rate, collision rate and coalescence efficiency kernels.		

Table 7: Typical equations solved along with Euler-Euler CFD model to predict drop size distribution by using method of moments [32].

$\frac{\partial m_k}{\partial t} + \nabla.(-D_T \nabla m_k + \overrightarrow{u_d} m_k) = S_k^{bb} + S_k^{bc} - S_k^{db} - S_k^{dc}$	The transport equation for k^{th} moment of the drop size distribution	(28)
$m_k = \int_0^{\infty} n(L)\, L^k dL$	Equation to evaluate k^{th} moment of the drop size distribution	(29)
$S_k^{bb} = \int_0^{+\infty} L^k \int_0^{+\infty} a(\lambda)\beta(L\|\lambda)n(\lambda)d\lambda dL$ $S_k^{bc} = \frac{1}{2}\int_0^{+\infty} n(\lambda) \int_0^{+\infty} h(q,\lambda)(q^3+\lambda^3)^{k/3}\, n(q)dqd\lambda$ $S_k^{db} = \int_0^{+\infty} L^k a(L)n(L)dL$ $S_k^{dc} = \int_0^{+\infty} L^k n(L) \int_0^{+\infty} h(L,\lambda)n(\lambda)d\lambda dL$	Source and sink terms of the transport equation of the k^{th} moment	(30)
$d_{32} = \frac{m_3}{m_2}$	Equation to obtain Sauter mean drop diameter from the moments of the drop size distribution.	(31)
m_k: k^{th} moment of drop size distribution; t: Time; D_T: Turbulent dispersion coefficient of the dispersed phase; $\overrightarrow{u_d}$: Dispersed phase velocity; S_k^{bb}: Source term for birth due to breakage; S_k^{bc}: Source term for birth due to coalesence; S_k^{db}: Sink term for death due to breakage; S_k^{dc}: Sink term for death due to coalesence; $a(L)$: Breakage rate of drops of diameter L; $h(q,\lambda)$: Coalescence rate of drops of diameter q and λ; $\beta(L\|\lambda)$: Distribution of daughter drops produced due to breakage of a drop of diameter λ; $n(L)$: Number of droplet of size L per unit volume; d_{32}: Sauter mean drop diameter.		

Table 8: Summary of some of the reported studies on CFD-PB modelling of solvent extraction equipment

Contactor	Turbulence model	PBM approach	Drag model	Objective
PSPC [30]	mixture *k–ε*	Method of classes	Kumar-Hartland	Estimation of d_{32} and dispersed phase holdup
PDDC [32]	mixture *k–ε*	Quadrature Method of Moments (QMOM)	Schiller–Naumann	Estimation of d_{32} and dispersed phase holdup
PSPC [33]	mixture *k–ε*	Method of classes	Modified Schiller-Naumann	Estimation of d_{32}, dispersed phase holdup and axial dispersion
PDDC [34]	mixture *k–ε*	Method of classes	Ishii-Zuber	Estimation of d_{32} and dispersed phase holdup. The breakage kernel obtained in a previous work by the authors was implemented in PBM.
PDDC [35]	mixture *k–ε*	Method of classes	Ishii-Zuber	Estimation of drop size distribution in PDDC after modifying PBM to account for the presence of liquid layer on wettable discs and doughnuts.
PDDC [36]	mixture *k–ε*	Method of classes	Ishii-Zuber	Determination of droplet breakup frequency and daughter droplet size distribution functions in a small computational domain using level-set method and subsequently implement them in a CFD-PBM of full-scale PDDC.
Pump-mixer [37]	mixture *k–ε*	Method of classes	Schiller-Naumann	Understanding the flow pattern and estimation of dispersed phase holdup and Sauter mean drop diameter
Continuous stirred settler [38]	mixture *k–ε*	QMOM	Morsi-Alexander	Estimation of dispersion band thickness
PDDC [39]	mixture *k–ε*	QMOM	Schiller-Naumann	Estimation of d_{32}
RDC [40]	mixture *k–ε*	Method of classes & QMOM	Schiller-Naumann	Estimation of d_{32} and dispersed phase holdup

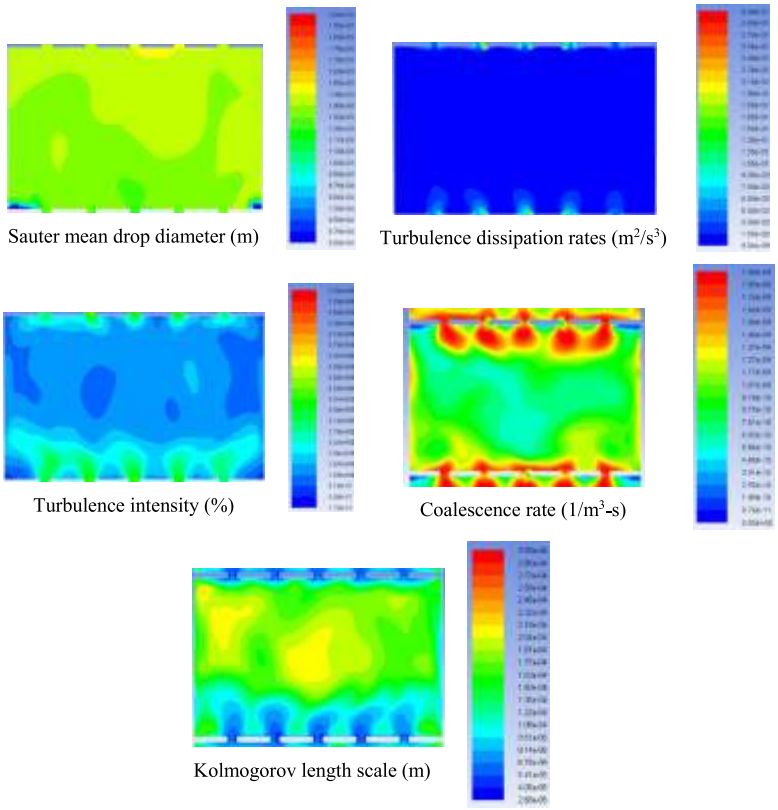

Table 8: Spatial variation of Sauter mean drop diameter, turbulence dissipation rate, turbulence intensity, coalescence rate and Kolmogorov length scale in an interplate space ($A_m f$ = 0.02 m/s; v_d = 0.004 m/s, v_c = 0.00207 m/s) "Reprinted from Progress in Nuclear Energy, 111, Nirvik Sen, K.K. Singh, A.W. Patwardhan, S. Mukhopadhyay, K.T. Shenoy, CFD-PBM simulations of a pulsed sieve plate column, 125-137, Copyright (2019), with permission from Elsevier".

used for CFD modelling in majority of these studies is Euler-Euler approach.

Interface tracking simulations of solvent extraction equipment

While most of the studies reported on CFD modelling of solvent extraction equipment can be classified in the categories described in the previous sections, there are several studies which do not fall in one of the above-mentioned categories. Though in most of the solvent extraction equipment, the flow is dispersed flow and the active volume of the equipment (the volume in which liquid-liquid dispersion is present) is known. However, in some equipment, the active volume is not constant but may vary depending on the operating conditions. Annular centrifugal extractor (ACE) is an example of such a contactor. In an ACE, the dispersion and mass transfer take place in the annular gap between a stator and a rotor. However, the volume present in the annular space is not fixed and may depend on several factors, the most important being the rotor speed and flow rates of the two liquid phases. To estimate liquid holdup in the annular gap, tracking of the free-surface (gas-liquid interface) in the annular gap is required. This can be done by using an interface tracking method like Volume of Fluid (VOF) method. There are several reported studies in which VOF model has been used for tracking the air-liquid interface in an ACE. Wardle and co-workers used VOF method to simulate gas-liquid flow in the annular gap of an annular centrifugal extractor considering only water as the liquid flowing through the centrifugal extractor [41]. Different turbulence models (RNG *k*- model, large eddy simulation method, and the detached eddy simulation) were compared. The experimental data was obtained using high-speed flow imaging and Laser Doppler Velocimetry (LDV) measurements. Subsequently, similar simulations to understand the effect of geometry of the mixing vanes at the bottom of the stationary bowl on hydrodynamics in ACE were reported. VOF method was used along with LES model of turbulence to track the air-water interface and capture turbulent flow field in the annular gap [42].

Recently, advanced computational approaches to simulate flow in solvent extraction equipment are being explored and reported. In a very recent study, the proof-of-concept of a novel modelling approach for ACE was reported [43]. This approach called GEneralized Multifluid Modelling Approach (GEMMA) is a hybrid approach which toggles between multifluid model (Euler-Euler type of model) and VOF kind of model for small-scale dispersed flow and large-scale segregated flow, respectively. One Secondary Particle Method (OSPM) was also coupled with CFD model.

Interface tracking simulations have also been reported for micro-scale solvent extraction contactors in which prediction of the flow regime (slug flow, droplet flow, parallel flow etc.) is important [44].

CFD modelling of mass transfer in solvent extraction equipment

Though the ultimate objective of a solvent extraction equipment is to ensure interphase mass transfer, most of the literature on CFD modelling of solvent extraction equipment is limited to flow simulations. The studies on CFD modelling of mass transfer in solvent extraction equipment, particularly, the ones which involve liquid-liquid dispersion are very few. While majority of large-scale solvent extraction equipment involve mass transfer in dispersive mode, equipment such as hollow fiber modules can be made to operate to achieve liquid-liquid mass transfer in non-dispersive mode. Two non-dispersive modes of operation of hollow fibre modules are solvent extraction mode and supported liquid membrane mode of operation. In solvent extraction mode of operation, the feed flows through the lumens of the hollow fiber whereas the solvent phase flows through the shell. The pores of the lumens are impregnated with the solvent phase flowing on the shell side. The solvent phase impregnated in the pores of the lumens facilitates mass transfer of the desired solute from the feed flowing in the lumen to the solvent flowing in the shell. In supported liquid mode of operation, the aqueous feed flows in the lumens and an aqueous strip phase flows in the shell side while the solvent phase fills the pores of the lumens of the hollow fibre. The mass transfer of the solute from the feed to the strip phase takes place through the solvent phase impregnated in the pores of the lumens. CFD modelling of mass transfer in hollow fibre module involves single-phase simulations of laminar flow of the aqueous phase and solvent/strip phase in the lumen and shell side, respectively. Mass transfer is simulated by solving convection-diffusion equations for the feed, shell sides and diffusion equation in the solvent phase impregnated in the pores of the lumen after applying complex boundary conditions of flux continuity and concentration jump at the feed side-lumen pore and lumen pore-shell side interfaces [45, 46]. Thus, the complexity in CFD simulation lies not in the governing equations but in implementation of the boundary conditions. As a result, the simulations of non-dispersive flow in hollow fibre are simpler than

simulations of dispersed flow in conventional solvent extraction equipment in which governing equations are complex but boundary conditions are simpler. Like hollow fibres, CFD modelling of mass transfer in microcontactors have also been reported. Such simulations typically involve a single entity (slug or drop) having continuous phase in its surrounding as the computational domain. Very small computational domain along with the fact that flow in a microcontactor is usually laminar make the simulations of liquid-liquid mass transfer in microcontactor relatively simpler. However, CFD modelling of mass transfer in conventional equipment which involve liquid-liquid dispersion are very few [47, 48]. This is primarily due to complexity in implementing additional species transport equations having source/ sink terms representing interphase mass transfer along with already complex flow equations and the equations of turbulence model. Also, such model requires overall mass transfer coefficient for which one of the several empirical models reported in literature can be used. The mass transfer prediction from the CFD model thus significantly depend on the choice of the mass transfer coefficient model.

As mentioned in the introduction section, some of solvent extraction equipment involve gas-liquid-liquid or gas-liquid-liquid-solid flows. Literature on CFD modelling of such solvent extraction equipment is practically non-existent.

Conclusions

The article provides an overview of approaches used for CFD modelling of solvent extraction equipment. Though the flow in a solvent extraction equipment is two-phase flow or multiphase flow, in some cases single-phase CFD modelling can provide useful data required for design. A pertinent example is design of pump-mix mixer in which single-phase CFD modelling can be used to design pump-mix impellers to meet the dual requirement of pumping and mixing in a mixer-settler cascade. Single-phase CFD simulation can also be used for performing virtual residence time distribution experiments to quantify and understand the deviation from ideal flow behaviour.

Two-phase CFD modelling of liquid-liquid dispersed flow assuming monodispersed droplets represents the next higher level of difficulty in CFD modelling of solvent extraction equipment. Euler-Euler method is the most widely used method whereas mixture k-ε model of turbulence is the most widely used model of turbulence for two-phase CFD modelling of solvent extraction equipment. The drag force is assumed to be the most important contributor to interphase momentum exchange. The results of CFD model may depend on the selection of drag model and this is the main source of empiricism in the two-phase CFD model of solvent extraction equipment.

Coupling of two-phase CFD modelling with population balance modelling leading to CFD-PB model is required if the assumption of constant diameter monodispersed drops is to be done away with to realistically model breakage and coalescence of drops which occur continuously in a solvent extraction equipment. Two approaches of population balance modelling – method of classes and method of moments – are briefly discussed. The flow field and drop size predicted by CFD-PB model depend on the models selected for breakage rate, coalescence rate and daughter droplet distribution and the values of the constants in these models. This necessitates a careful selection of these models and validation of CFD-PB model with experimental data.

While above-mentioned modelling approaches cover the vast majority of studies on CFD modelling of solvent extraction equipment, some special class of equipment such as annual centrifugal extractors which do not have fixed active volume or microcontactors in which dispersed phase may have size of the order of the diameter of the contactor may require interface tracking simulations. Such simulations are briefly discussed.

Though the ultimate objective of using a solvent extraction equipment is to achieve mass transfer, CFD modelling of mass transfer in solvent extraction equipment are scant. This is attributed to the complexities introduced due to solution of additional equations required to model mass transfer and also in conducting mass transfer experiments which require once through flow unlike the flow experiments which are generally closed loop. However, CFD modelling of mass transfer in equipment which work on the principle of non-dispersive flow such as hollow fibre contactor or microcontactors, in which it is possible to simulate mass transfer with a single entity of the dispersed phase (e.g. a single slug or droplet) rather than a swarm of dispersed phase entities, have been reported. This is due to significant reduction in the complexity of the governing equations to be solved or reduction in the size of the computational domain.

Like in any other field, advances in the field of CFD modelling of solvent extraction are taking place such as development of hybrid models suitable for multiscale flows as in an annular centrifugal extractor, reduced population balance model to make computations faster and fundamental understanding of the phenomena of drag, droplet breakage, droplet coalescence in the quest for minimizing empiricism in equipment level CFD modelling.

Corresponding Author*

K.K. Singh (kksingh@barc.gov.in)

References

[1] H. Singh, and C.K. Gupta, *Mineral Processing and Extractive Metullargy Review*, 2000, **21**,**(1-5)**, 307.

[2] R. Natarajan, *Progress in Nuclear Energy*, 2017, **101**, 118.

[3] P. Sinharoy, D. Banerjee, S. Manohar, and C.P. Kaushik, *Separation Science and Technology*, 2021, **56(8)**, 1450-1456.

[4] S. Manohar, J.N. Sharma, B.V. Shah, and P.K. Wattal, *Nuclear Science and Engineering*, 2007, **156(1)**, 96-102.

[5] N.V. Thakur, *Mineral Processing and Extractive Metullargy Review, 2000*, **21**(1-5), 277-306.

[6] K.K. Singh, K.T. Shenoy, A.K. Mahendra, and S.K. Ghosh, *Chemical Engineering Science*, 2004, **59(14)**, 2937-2945.

[7] K.K. Singh, S.M. Mahajani, K.T. Shenoy, and S.K. Ghosh, *AIChE Journal*, 2008, **54(1)**, 42-55.

[8] A. Brucato, M. Ciofalo, F. Grisafi, and G. Micale, *Chemical Engineering Science* 1998, **53(21)**, 3653-3684.

[9] S. Sarkar, K.K. Singh, and K.T. Shenoy, *Separation Science and Technology*, 2017, **52(18)**, 2863-2877.

[10] S. Sarkar, K.K. Singh, and K.T. Shenoy, *Progress in Nuclear Energy*, 2018, **106**, 335-344.

[11] S. Sarkar, K.K. Singh, and K.T. Shenoy, *Chemical Engineering and Processing-Process Intensification*, 2020, **155**, 108052.

[12] N. Sen, K.K. Singh, A.W. Patwardhan, S. Mukhopadhyay, and K.T. Shenoy, *Separation Science and Technology*, 2015, **50(16)**, 2485-2495.

[13] K.K. Singh, S.M. Mahajani, K.T. Shenoy, A.W. Patwardhan, and S.K. Ghosh, *Chemical Engineering Science*, 2007, **62**, 1308-1322.

[14] K.K. Singh, S.M. Mahajani, K.T. Shenoy, and S.K. Ghosh, *Industrial and Engineering Chemistry Research*, 2007, **46**, 2180-2190.

[15] C. Drumm, and H.-J. Bart, *Chemical Engineering and Technology*, 2006, **29(11)**, 1297-1302.

[16] A. Amokrane, S. Charton, F. Lamadie, J.F. Paisant, and F. Puel, *Chemical Engineering Science*, 2014, **114**, 40-50.

[17] M.A. Nabli, P. Guiraud, and C. Gourdon, *Chemical Engineering Science*, 1997, **52(14)**, 2353-2368.

[18] N. Sen, K.K. Singh, A.W. Patwardhan, S. Mukhopadhyay, and K.T. Shenoy, *Separation Science and Technology*, 2016, **51(17)**, 2790-2803.

[19] N. Sen, K.K. Singh, A.W. Patwardhan, S. Mukhopadhyay, and K.T. Shenoy, *Separation Science and Technology*, 2018, **53**(16), 2587-2600.

[20] S. Sarkar, K.K. Singh, and K.T. Shenoy, *Separation and Purification Technology*, 2019, **209**, 608-622.

[21] S. Sarkar, K.K. Singh, and K.T. Shenoy, *Industrial & Engineering Chemistry Research,* 2019, **58(33)**, 15307-15320.

[22] X. Yu, H. Zhou, S. Jing, W. Lan, and S. Li, *Solvent Extraction and Ion Exchange*, 2018, **36(5)**, 480-498.

[23] X. Yu, H. Zhou, Q. Zheng, S. Jing, W. Lan, and S. Li, *Chinese Journal of Chemical Engineering*, 2020, **28(6)**, 1504-1513.

[24] R.A. Farakte, N.V. Hendre, and A.W. Patwardhan, *Industrial & Engineering Chemistry Research*, 2018, **57(50)**, 17192-17208.

[25] F. Onink, C. Drumm, G.W. Meindersma, H.-J. Bart, and A.B. de Haan, *Chemical Engineering Journal*, 2010, **160(2)**, 511-521.

[26] H. Yi, K.H. Smith, W. Fei, and G.W. Stevens, *Solvent Extraction and Ion Exchange*, 2020, **38(1)**, 88-102.

[27] K.K. Singh, S.M. Mahajani, K.T. Shenoy, and S.K. Ghosh, *Industrial and Engineering Chemistry Research*, 2009, **48(17)**, 8121-8133.

[28] S. Alzyod, M. Attarakih, A. Hasseine, and H.-J. Bart, *Chemical Engineering Research and Design*, 2017, **117**, 549-556.

[29] S. Alzyod, M. Attarakih, and H.-J. Bart, *Computer Aided Chemical Engineering*, 2018, **43**, 451-456.

[30] N. Sen, K.K. Singh, A.W. Patwardhan, S. Mukhopadhyay, and K.T. Shenoy, *Progress in Nuclear Energy*, 2019, **111**, 125-137.

[31] M.A. Hsia, and L.L. Tavlarides, *The Chemical Engineering Journal*, 1980, **20(3)**, 225-236.

[32] S. Sarkar, K.K. Singh, S.M. Mahajani, and K.T. Shenoy, *Solvent Extraction and Ion Exchange*, 2020, **38(5)**, 536-554.

[33] N. Sen, K.K. Singh, A.W. Patwardhan, K.T. Shenoy, *Solvent Extraction and Ion Exchange*, 2021, **39(3)**, 328-352.

[34] X. Yu, H. Zhou, S. Jing, W. Lan, and S. Li, *Chemical Engineering Science*, 2019, **201**, 349-361.

[35] X. Yu, H. Zhou, S. Jing, W. Lan, and S. Li, *Industrial and Engineering Chemistry Research*, 2020, **59(17)**, 8436-8446.

[36] X. Yu, H. Zhou, S. Jing, W. Lan, and S. Li, *Chemical Engineering Science*, 2020, **226**, 115851.

[37] H. Zhou, X. Yu, B. Wang, S. Jing, W. Lan, and S. Li, *Industrial and Engineering Chemistry Research*, 2021, **60(4)**, 1926-1938.

[38] X.H. Guo, Q.Y. Zhao, T.A. Zhang, Z.M. Zhang, and S. Zhu, *JOM*, 2019, **71(5)**, 1650-1659.

[39] A. Amokrane, S. Maaß, F. Lamadie, F. Puel, and S. Charton, *Chemical Engineering Journal*, 2016, **296**, 366-376.

[40] C. Drumm, M. Attarakih, and H.-J. Bart, *Chemical Engineering Science*, 2009, **64(4)**, 721-732.

[41] K.E. Wardle, T.R. Allen, M.H. Anderson, M.H., and R.E. Swaney, *AIChE Journal*, 2008, **54(1)**, 74-85.

[42] K.E. Wardle, T.R. Allen, M.H. Anderson, and R.E. Swaney, *AIChE Journal*, 2009, **55(9)**, 2244-2259.

[43] A.D. Santis, B.C. Hanson, M. Fairweather, *Chemical Engineering Science*, 2021, **242**, 116729.

[44] R. Filimonov, Z. Wu, and B. Sundén, *Chemical Engineering Research and Design*, 2021, **166**, 135-147.

[45] B. Swain, K.K. Singh, and A.K. Pabby, *Separation Science and Technology*, 2021, **56(16)**, 2848-2863.

[46] B. Swain, K.K. Singh, and A.K. Pabby, *Solvent Extraction and Ion Exchange*, 2019, **37(7)**, 526-544.

[47] N. Sen, K.K. Singh, A.W. Patwardhan, S. Mukhopadhyay, and K.T. Shenoy, CFD modelling to predict mass transfer in pulsed sieve plate extraction columns, 12th International Conference on Computational Fluid Dynamics in the Oil & Gas, Metallurgical and Process Industries (CFD-2017), 30 May-June 1 (2017), Trondheim, Norway.

[48] X. Yu, H. Zhou, S. Jing, W. Lan, and S. Li, *Chemical Engineering Science*, 2021, **230**, 116184.